

Quantum Dropout for Efficient Quantum Approximate Optimization Algorithm on Combinatorial Optimization Problems

Zhen-Duo Wang,¹ Pei-Lin Zheng,¹ Biao Wu,^{1, 2, 3} and Yi Zhang^{1, 3, *}

¹International Center for Quantum Materials, School of Physics, Peking University, Beijing 100871, China

²Wilczek Quantum Center, School of Physics and Astronomy,

Shanghai Jiao Tong University, Shanghai 200240, China

³Collaborative Innovation Center of Quantum Matter, Beijing 100871, China

A combinatorial optimization problem becomes very difficult in situations where the energy landscape is rugged and the global minimum locates in a narrow region of the configuration space. When using the quantum approximate optimization algorithm (QAOA) to tackle these hard cases, we find that difficulty mainly originates from the QAOA quantum circuit instead of the cost function. To alleviate the issue, we selectively drop out the clauses defining the quantum circuit while keeping the cost function intact. Due to the combinatorial nature of the optimization problems, the dropout of clauses in the circuit does not affect the solution. Our numerical results confirm QAOA's performance improvements with various types of quantum-dropout implementation.

Introduction—A class of important real-world optimization problems, including NP-complete or NP-hard problems, cost exponential resources to solve on a classical computer [1–3]. As the size of the problem increases, a solution becomes so costly that it is virtually impossible for even the world's largest supercomputers. Although quantum computers have been shown to hold enormous advantages over classical computers on some specific problems [4–8], an important open question is whether a quantum computer can provide advantages and improve our stance on these difficult optimization problems.

The quantum approximate optimization algorithm (QAOA) is a hybrid quantum-classical variational algorithm designed to tackle ground-state problems, especially discrete combinatorial optimization problems [9–22]. It has been shown quite effective in many problems. However, we note that these studies mainly focus on randomly generated problems [9–13], which may concentrate on simpler cases and fail to represent the problem's categorical difficulty. In this work, we try to address these difficult cases with a strategy we call quantum dropout.

We focus on combinatorial optimization problems where the global minimum (ground state) \mathbf{s}_{gs} has to satisfy each clause \hat{H}_{c_i} in a given set C ,

$$\hat{H}_C = \sum_{c_i \in C} \hat{H}_{c_i}. \quad (1)$$

The difficulty of this problem depends on the energy landscape. As illustrated in Fig. 1(a), when the global minimum locates in a large and smooth neighborhood, the problem is simple since its solution can be efficiently found with local-based searches such as simulated annealing (SA) [23] and the greedy algorithm [24]. When the minimum locates in a narrow region in a rugged landscape, the case is hard. This is further demonstrated in Figs. 1(b) and 1(c), which are the energy landscapes of simple and hard cases in the not-all-equal

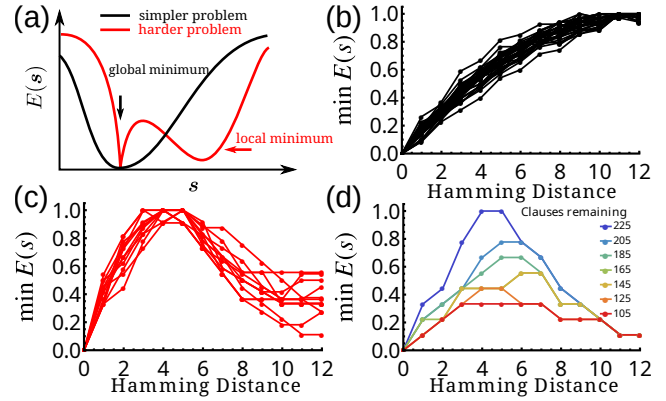


FIG. 1: (a) A schematic energy landscape. The global minimum is located in a large and smooth neighborhood for a simple problem and a narrow region for a hard problem. Normalized landscapes for NAE3SAT problems in terms of the hamming distance: (b) for simple cases and (c) for hard cases. (d) The landscape of a hard problem becomes smoother as more clauses are dropped out, improving the global minimum's standing. Only the minimum of $E(s)$ for a specific hamming distance s from the global minimum is shown for clarity. $N = 24$.

3-SAT (NAE3SAT) problems [25, 26], respectively. Figs. 1(d) shows that the energy landscape for hard cases becomes much smoother as more clauses are dropped out. This observation, combined with the realization that a more rugged landscape makes the quantum circuit more costly, leads us to a strategy, where we choose to drop out a portion of clauses from the quantum circuit, $\hat{H}_{C'} = \sum_{c_i \in C' \subset C} \hat{H}_{c_i}$, while keeping the original cost function to ensure the uniqueness of the global minimum. This strategy, as illustrated schematically in Fig. 2, has no parallel in classical algorithms and utilizes the problems' combinatorial nature. Our numerical results show

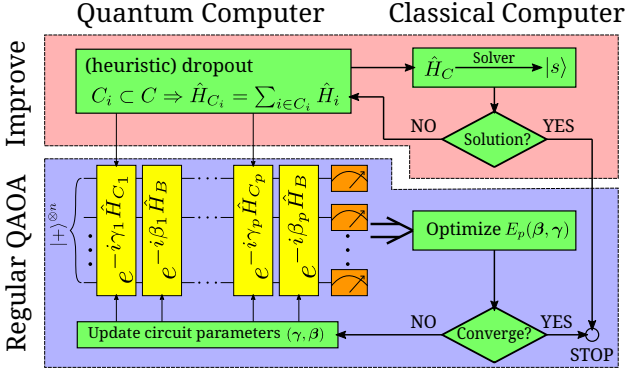


FIG. 2: QAOA is a hybrid optimization procedure that consists of a $2p$ -layer quantum circuit evaluating a cost function and a classical algorithm optimizing the corresponding parameters β, γ . Each bi-layer contains a driving layer ($e^{-i\hat{H}_C\gamma_m}$) and a mixing layer ($e^{-i\hat{H}_B\beta_m}$), where m is the bi-layer index. In addition, we propose to check the target problem with classical algorithms first to see whether QAOA is necessary and implement a dropout on the \hat{H}_C clauses presenting in each of the driving layers.

that with quantum dropout QAOA can locate the ground states with an enhanced probability and little to no overhead even for hard cases, paving the way towards practical QAOA for combinatorial optimizations. In the deep artificial neural network, there is a vital technique called dropout, which keeps a random subset of neurons from optimization for more independent neurons and thus suppresses over-fitting [27, 28]. Our quantum dropout echoes this classical technique in spirit but is not a direct generalization.

QAOA and quantum dropout—QAOA was proposed to solve optimization problems such as Eq. 1 by finding its ground state $|s_{gs}\rangle$, which is one of the N -qubit basis $|\mathbf{s}\rangle$ over the σ^z configurations: $\sigma_i^z|\mathbf{s}\rangle = s_i|\mathbf{s}\rangle$. As shown in Fig. 2, QAOA offers a parameterized variational state:

$$|\beta, \gamma\rangle = e^{-i\hat{H}_B\beta_p} e^{-i\hat{H}_{C_p}\gamma_p} \cdots e^{-i\hat{H}_B\beta_1} e^{-i\hat{H}_{C_1}\gamma_1} |+\rangle^{\otimes n}, \quad (2)$$

where $\hat{H}_B = -\sum_i \sigma_i^x$ with $|+\rangle^{\otimes n}$ being its ground state. In Ref. [9], the original setup is inspired by quantum adiabatic (annealing) algorithm [29–31] such that $\hat{H}_{C_1} = \cdots \hat{H}_{C_p} = \hat{H}_C$. QAOA implements a quantum circuit to efficiently evaluate the expectation value of Eq. 2 as a cost function:

$$C(\beta, \gamma) = \langle \beta, \gamma | \hat{H}_C | \beta, \gamma \rangle, \quad (3)$$

which is in turn optimized classically. The quantum circuit evaluates an exponential number of classical configurations simultaneously, and with more layers the overlap $\langle s_{gs} | \beta, \gamma \rangle$ becomes larger. At the convergence, $|\beta, \gamma\rangle$ is measured in the basis of $\{|\mathbf{s}\rangle\}$.

In comparison with variational quantum eigensolver [32–34], QAOA possesses far fewer variational parameters - basically, the $2p$ variables of β, γ . Usually, we need $p \gtrsim O(N)$ for sufficient expressing power of $|\beta, \gamma\rangle$ to encode \mathbf{s}_{gs} [35]; however, a larger p complicates the non-convex optimization of $C(\beta, \gamma)$ [20, 36–39], especially for quantum circuits with hard \hat{H}_C , as we will see later. May we swap \hat{H}_C for a simpler one in the quantum circuit? Unfortunately, the answer is negative - a quantum circuit with $\hat{H}_{C'}$ generally does not apply to the problem of a different \hat{H}_C . Intuitively, the QAOA quantum circuit performs as an interferometer, where only \mathbf{s} at the minimums of \hat{H}_C interfere constructively through the $e^{-i\hat{H}_C x_m}$ driving layers [40]. We will illustrate related numerical examples later and in Supplemental Materials. It may be viable to apply a simpler $\hat{H}_{C'}$ that share the same \mathbf{s}_{gs} with \hat{H}_C ; however, this is generally unpractical as the required \mathbf{s}_{gs} is unknown beforehand.

Fortunately, for combinatorial optimization problems, the Hamiltonian $\hat{H}_{C'} = \sum_{c_i \in C'} \hat{H}_{c_i}$ with a partial set $C' \subset C$ offers an answer. As we mentioned earlier, dropping out clauses improves the energy landscape of a harder problem while ensuring \mathbf{s}_{gs} being the ground state of $\hat{H}_{C'}$. The caveat is, in addition to \mathbf{s}_{gs} , there could be false solutions due to the now fewer constraints. To avoid the false solutions, we substitute these simpler problems $\hat{H}_{C_1, \dots, p}$ into Eq. 2 while keeping the cost function in Eq. 3.

Let us summarize our improvements to the regular QAOA via quantum dropout (Fig. 2). We start the problem with an efficient classical solver. If the result is satisfactory, we stop the procedure since there is no point in a quantum solver. Otherwise, these failed classical results, typically low-lying excited states (local minima), offer insights as we prepare quantum dropout for QAOA: whether a clause should be kept or available for quantum dropout to underweight the distractions and enhance the chances to locate \mathbf{s}_{gs} . Finally, we optimize $|\beta, \gamma\rangle$ with respect to the original cost function $\langle \hat{H}_C \rangle$ with a complete set of clauses to ensure the uniqueness of the global minimum. The current procedure does not incur obvious overhead to the conventional QAOA since the preliminary approaches and the quantum-dropout controls are both inexpensive on a classical computer. We leave further details to the later examples and Supplemental Materials.

Not-all-equal 3-SAT problems—Without loss of generality, we use this specific combinatorial problem to illustrate how to implement QAOA with quantum dropout and demonstrate its effectiveness. The solution \mathbf{s}_{gs} of an NAE3SAT problem satisfies not-all-equal s_i, s_j, s_k for a given set of clauses $[i, j, k] \in \mathcal{C}$. For instance, clause $[1, 2, 3]$ allows $s_1 = s_2 = 1, s_3 = -1$ but not $s_1 = s_2 = s_3 = 1$. Such NAE3SAT problems are NP-complete and a polynomial algorithm is not yet available

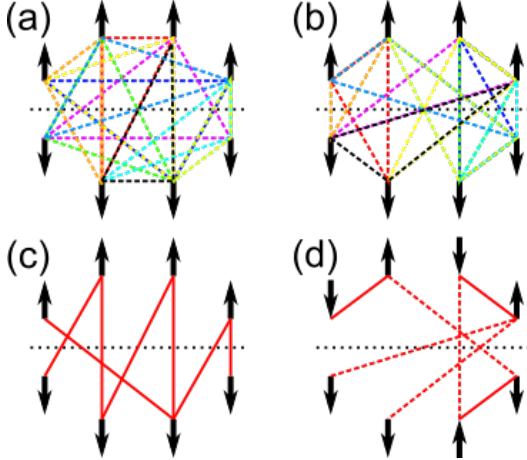


FIG. 3: (a) and (b): The NAE3SAT problem with 10 clauses over $N = 8$ spins is simpler (harder) when the clauses are more sporadic (concentrated on a few pairs). Each color denotes a different clause, which must traverse the central dotted line for the not-all-equal condition. (c) and (d): a step-by-step local analysis first follows the strongest antiferromagnetic interactions (red lines), then the second strongest (red dashed lines), and so forth. While the result for the simpler problem is consistent with s_{gs} , the result for the harder problem largely misleads.

in general [2, 25, 26, 41].

The solution of an NAE3SAT problem is the ground state of the following Hamiltonian

$$\begin{aligned} \hat{H}_C &= \sum_{[i,j,k] \in C} \left[(s_i + s_j + s_k)^2 - 1 \right] / 2 \\ &= \sum_{[i,j,k] \in C} (s_i s_j + s_i s_k + s_j s_k) + \text{const.}, \end{aligned} \quad (4)$$

where the interaction between a pair of Ising spins $s_i s_j$ is antiferromagnetic, and its strength depends on the number of times i and j appear in pairs within all clauses. A clause favors antiferromagnet as it imposes two opposite and only one parallel alignment. Therefore, a straightforward and physically intuitive solution is to anti-align the pair of spins with the most appearances in clauses, then the pair with the second most appearances, and so forth, in analogy with the greedy algorithm (Fig. 3c) [24]. However, if such a local perspective yields globally inconsistent deductions with s_{gs} , e.g., multiple pairs of spins with repeated appearances in clauses are counter-intuitively aligned, see Figs. 3b and 3d, the NAE3SAT problem is commonly harder. We emphasize that these challenging problems, despite their restrictive guidelines and thus overshadowed percentage by random problems (Fig. 3a), determine the categorical complexity and are more meaningful from a quantum-solver perspective.

Following these guidelines in Fig. 3 for simpler or

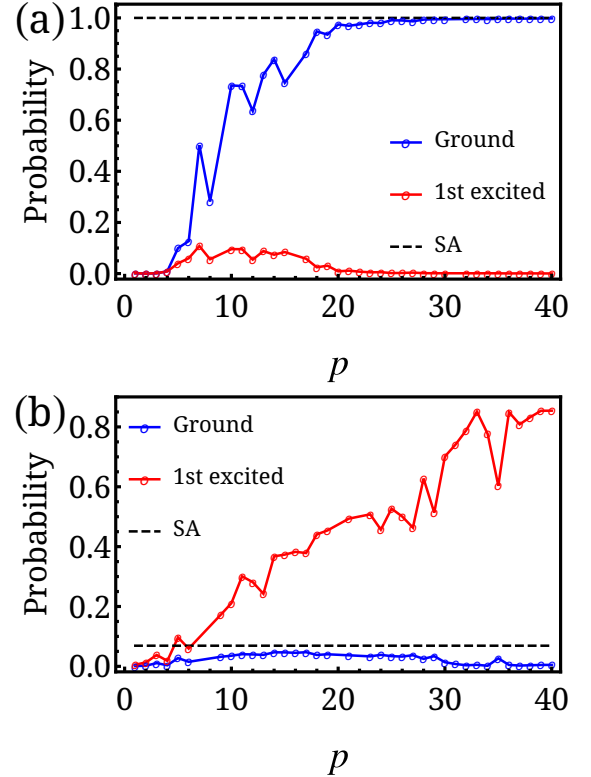


FIG. 4: We use the probability of achieving the ground state s_{gs} as a measure of the performance of QAOA and SA on an (a) simpler and (b) harder NAE3SAT problem of system size $N = 16$. While QAOA performs satisfactorily on the simpler problem \hat{H}_C^E , especially for sufficient circuit depth p , it faces challenges on the harder problem \hat{H}_C^H and performs no better than SA. We estimate the SA success probability over 1000 trials.

harder problems, respectively, we generate NAE3SAT problems starting from s_{gs} and accumulating consistent clauses \hat{H}_{c_i} until the ground state of \hat{H}_C is unique (other than a global $s_i \rightarrow -s_i$ symmetry). To quantify each problem's difficulty, we evaluate the chance R of finding s_{gs} in Monte Carlo simulated annealing (SA) [23], with $R > 95\%$ for most problems following Fig. 3a, and $R < 10\%$ for selected problems following Fig. 3b [42]. The qualitative nature of the energy landscapes of such problems, as well as the effects of quantum dropout, have been illustrated previously in Fig. 1. Next, we examine our numerical results on QAOA on these NAE3SAT problems.

Results —First, we apply regular QAOA on typical simpler and harder NAE3SAT problems, whose results are summarized in Fig. 4. Indeed, QAOA is successful on a simpler problem \hat{H}_C^E , with the ground state's weight tending to 100% as the circuit depth increases; however, such success is less exciting as SA also achieves s_{gs} with a high probability of $\sim 100\%$. On the other hand, QAOA

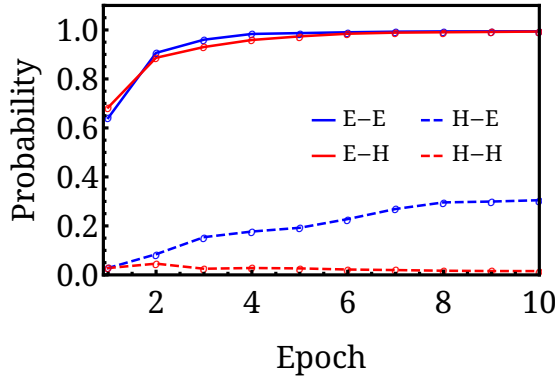


FIG. 5: We evaluate the QAOA performance with $p = 30$ via the probability of achieving the ground state \mathbf{s}_{gs} as we graft the quantum circuit of \hat{H}'_C to the cost function of \hat{H}_C , where \hat{H}'_C and \hat{H}_C can each be a simpler problem \hat{H}_C^E or a harder problem \hat{H}_C^H with the same \mathbf{s}_{gs} . The horizontal axis labels the optimization epochs. The legend $X - Y$ denotes \hat{H}_C^X for the quantum circuit and \hat{H}_C^Y for the cost function, where $X, Y = E, H$.

performs no better than SA on a harder problem \hat{H}_C^H , and to make the matter worse, a deeper circuit hardly improves its performance and may even become harmful, as more and more weights get stuck in low-lying excited states. These behaviors are general to other simpler and harder problems as well.

As the problem difficulty, and more fundamentally, its energy landscape enters QAOA from both the (driving layers of) quantum circuit and the cost function aspects, we study their relative impact by assigning different yet consistent problems to the quantum circuit and the cost function. We have reasoned previously that \mathbf{s}_{gs} needs to be consistent between the quantum circuit and the cost function and show failure examples due to the incompatibility in the Supplemental Materials. Here, we perform a cross test, where the problem \hat{H}'_C used in the quantum circuit may differ from \hat{H}_C in the cost function, and $\hat{H}'_C, \hat{H}_C = \hat{H}_C^E, \hat{H}_C^H$, the simpler and harder problems studied in Fig. 4. We summarize the convergence of $|\beta, \gamma\rangle$ towards $|\mathbf{s}_{gs}\rangle$ in Fig. 5 as a measure of QAOA performance. The QAOA performs overwhelmingly well as long as the quantum circuit engages a simpler problem $\hat{H}'_C = \hat{H}_C^E$, and vice versa, while the cost function \hat{H}_C plays a relatively minor role, which demonstrates that the quantum circuits is the bottleneck and should be our main target of simplification.

As discussed earlier, quantum dropout rightfully addresses such concerns on QAOA quantum circuits, providing us with simpler yet still compatible \hat{H}'_C for the driving layers. As we checked the difficulty of the harder problem \hat{H}_C^H via SA in Fig. 4, we have also obtained, as a by-product, 29 low-lying excited states, which help us to

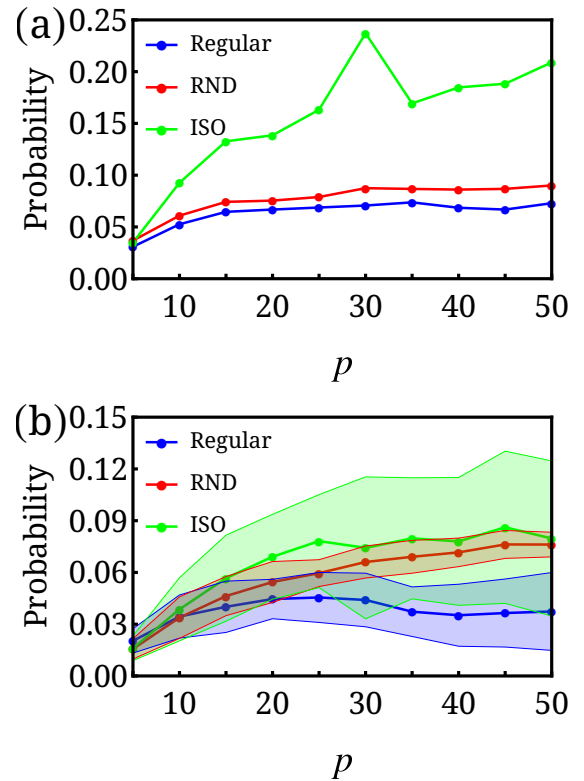


FIG. 6: By the success probability versus the model depth p of (a) the best case and (b) the averages and standard deviations over the trials, we compare the performance of QAOA of three forms: the regular QAOA (blue line), the QAOA with a quantum dropout of an identical \hat{H}'_C (green line) or different $\hat{H}_{C_1, \dots, p}$ (red line) over the driving layers. For each trial, we randomize the initial parameters (β, γ) among $(-\pi, \pi)^{\otimes 2p}$, and for the QAOA with quantum dropout, the clauses for the dropout Hamiltonians. The number of trials varies according to p , $p \leq 20$: 100, $25 \leq p \leq 40$: 50, and $45 \leq p$: 30.

choose the dropout clauses more selectively. For example, we only implement quantum dropout on clauses that observe no violation with these distractions here, and we leave further results and discussions on the effect of such selections to Supplemental Materials. The resulting energy landscape was previously illustrated in Fig. 1d. We leave the cost function $\hat{H}_C = \hat{H}_C^H$ intact with all of the clauses and perform the QAOA optimization following the procedure in Fig. 2.

First, we set identical quantum dropout, randomly selected 50% of the clauses in the available subset, to all driving layers, i.e., $\hat{H}_{C_1} = \hat{H}_{C_2} = \dots = \hat{H}_{C_p}$. The QAOA performance is shown as the green lines in Fig. 6. We observe an evident improvement in favor of the quantum dropouts, which becomes more significant as the circuit depth p grows. At $p = 50$, the QAOA's probability of

locating the ground state doubles on average with the implementation of the quantum dropouts, with the best-case scenario offering a success probability of ~ 0.21 , well exceeding that of ~ 0.073 for the regular QAOA and the SA probability of ~ 0.069 . Intuitively, when p is small, the limiting factor is the quantum circuit's capacity; as p and thus quantum circuit's expressibility increases, the bottleneck switches to the optimization of the variational parameters, where the regular QAOA commonly gets bogged down and the quantum dropout begins to shine (see the averaged performance in Fig. 6b).

We also examine the scheme of setting driving layers with different dropouts. Our motivation is two-fold: first, we want to suppress the performance variance; more interestingly, different dropouts lead to different landscapes, therefore, s_{gs} and only s_{gs} , the intersection between the minimums of $\hat{H}_{C'}$ with all possible dropouts, may interfere constructively through all driving layers and remain stand-out. The corresponding result is summarized in the red lines in Fig. 6, suggesting this scheme's improvement over the regular QAOA at sufficiently large p . We observe a lower performance variance compared with the uniform quantum dropout, though there is no apparent difference, on average, at the current limit of system size ($N = 16$) and circuit depth ($p = 50$). If only a limited number of trials are available, this dropout architecture is advisable for its consistent performance exceeding SA. Besides, we have studied soft quantum dropout, where we allow each clause to contribute to $\hat{H}_{C'}$ in variable percentages instead of the binary assignment of in or out. In theory, this setup may ravel up the spectrum leading to more destructive and inconsistent interference through the driving layers for the low-lying excited states. However, we have not observed numerical evidence supporting its advantages yet.

Discussions—In summary, we have illustrated that while the regular QAOA performs satisfactorily on simpler problems, it still faces significant challenges on meaningful, harder problems. The benefit of a straight increase of the circuit depth quickly saturates, with most of the weights trapped in low-lying excited states. Correspondingly, we have proposed a quantum-dropout strategy for QAOA on harder combinatorial optimization problems, which keep a number of clauses out of their role in the quantum circuits, therefore easing the landscape of the problem and thus the parameter optimization. The strategy provides an edge over the regular QAOA and classical methods such as SA. For best performance, multiple (quantum dropout) setups and (parameter) initializations should be attempted. Our study also provides valuable insight into the mechanism of QAOA.

Finally, in addition to the classical combinatorial optimizations such as the NAE3SAT problems, the physical picture for problems' simpler-harder dichotomy and QAOA with quantum dropout straightforwardly apply towards quantum combinatorial optimizations, such as

Eq. 1 with \hat{H}_{ci} no longer commuting with each other and a target ground state $|s_{gs}\rangle$ individually satisfying (the ground-state condition for) each \hat{H}_{ci} ; see examples in Supplemental Materials. Such quantum many-body problems lack a general, compatible classical solver, making the efficient QAOA assisted by quantum dropout very useful under the circumstances.

Acknowledgement: We thank Jia-Bao Wang for insightful discussions. YZ and PZ are supported by the National Science Foundation of China (No.12174008). ZW and BW are supported by the National Key R&D Program of China (Grants No. 2017YFA0303302, No. 2018YFA0305602), National Natural Science Foundation of China (Grant No. 11921005), and Shanghai Municipal Science and Technology Major Project (Grant No.2019SHZDZX01). The calculations of this work is supported by HPC facilities at Peking University.

* frankzhangyi@gmail.com

- [1] R. E. Ladner, J. ACM **22**, 155–171 (1975).
- [2] M. R. Garey and D. S. Johnson, *Computers and Intractability: A Guide to the Theory of NP-Completeness* (W. H. Freeman & Co., USA, 1990).
- [3] S. Aaronson, SIGACT News **36**, 30–52 (2005).
- [4] P. W. Shor, SIAM Review **41**, 303 (1999), <https://doi.org/10.1137/S0036144598347011>.
- [5] A. W. Harrow and A. Montanaro, Nature **549**, 203 (2017).
- [6] S. Bravyi, D. Gosset, and R. König, Science **362**, 308 (2018).
- [7] F. Arute, K. Arya, R. Babbush, D. Bacon, J. C. Bardin, R. Barends, R. Biswas, S. Boixo, F. G. S. L. Brandao, D. A. Buell, B. Burkett, Y. Chen, Z. Chen, B. Chiaro, R. Collins, W. Courtney, A. Dunsworth, E. Farhi, B. Foxen, A. Fowler, C. Gidney, M. Giustina, R. Graff, K. Guerin, S. Habegger, M. P. Harrigan, M. J. Hartmann, A. Ho, M. Hoffmann, T. Huang, T. S. Humble, S. V. Isakov, E. Jeffrey, Z. Jiang, D. Kafri, K. Kechedzhi, J. Kelly, P. V. Klimov, S. Knysh, A. Korotkov, F. Kostritsa, D. Landhuis, M. Lindmark, E. Lucero, D. Lyakh, S. Mandrà, J. R. McClean, M. McEwen, A. Megrant, X. Mi, K. Michelsen, M. Mohseni, J. Mutus, O. Naaman, M. Neeley, C. Neill, M. Y. Niu, E. Ostby, A. Petukhov, J. C. Platt, C. Quintana, E. G. Rieffel, P. Roushan, N. C. Rubin, D. Sank, K. J. Satzinger, V. Smelyanskiy, K. J. Sung, M. D. Tervitthick, A. Vainsencher, B. Villalonga, T. White, Z. J. Yao, P. Yeh, A. Zalcman, H. Neven, and J. M. Martinis, Nature **574**, 505 (2019).
- [8] H.-S. Zhong, H. Wang, Y.-H. Deng, M.-C. Chen, L.-C. Peng, Y.-H. Luo, J. Qin, D. Wu, X. Ding, Y. Hu, P. Hu, X.-Y. Yang, W.-J. Zhang, H. Li, Y. Li, X. Jiang, L. Gan, G. Yang, L. You, Z. Wang, L. Li, N.-L. Liu, C.-Y. Lu, and J.-W. Pan, Science **370**, 1460 (2020).
- [9] E. Farhi, J. Goldstone, and S. Gutmann, “A quantum approximate optimization algorithm,” (2014), arXiv:1411.4028 [quant-ph].
- [10] L. Zhou, S.-T. Wang, S. Choi, H. Pichler, and M. D.

- Lukin, Phys. Rev. X **10**, 021067 (2020).
- [11] P. Vikstål, M. Grönkvist, M. Svensson, M. Andersson, G. Johansson, and G. Ferrini, Phys. Rev. Applied **14**, 034009 (2020).
- [12] M. Willsch, D. Willsch, F. Jin, H. De Raedt, and K. Michielsen, Quantum Information Processing **19**, 197 (2020).
- [13] V. Akshay, H. Philathong, M. E. S. Morales, and J. D. Biamonte, Phys. Rev. Lett. **124**, 090504 (2020).
- [14] W. W. Ho and T. H. Hsieh, SciPost Phys. **6**, 29 (2019).
- [15] G. Pagano, A. Bapat, P. Becker, K. S. Collins, A. De, P. W. Hess, H. B. Kaplan, A. Kyprianidis, W. L. Tan, C. Baldwin, L. T. Brady, A. Deshpande, F. Liu, S. Jordan, A. V. Gorshkov, and C. Monroe, Proceedings of the National Academy of Sciences **117**, 25396 (2020).
- [16] M. Streif and M. Leib, Quantum Science and Technology **5**, 034008 (2020).
- [17] S. H. Sack and M. Serbyn, Quantum **5**, 491 (2021).
- [18] M. Medvidovic and G. Carleo, npj Quantum Information **7**, 101 (2021).
- [19] J. Villalba-Diez, A. González-Marcos, and J. B. Ordieres-Meré, Sensors **22** (2022), 10.3390/s22010244.
- [20] L. Bittel and M. Kliesch, Phys. Rev. Lett. **127**, 120502 (2021).
- [21] G. Matos, S. Johri, and Z. Papić, PRX Quantum **2**, 010309 (2021).
- [22] M. P. Harrigan, K. J. Sung, M. Neeley, K. J. Satzinger, F. Arute, K. Arya, J. Atalaya, J. C. Bardin, R. Barends, S. Boixo, M. Broughton, B. B. Buckley, D. A. Buell, B. Burkett, N. Bushnell, Y. Chen, Z. Chen, B. Chiaro, R. Collins, W. Courtney, S. Demura, A. Dunsworth, D. Eppens, A. Fowler, B. Foxen, C. Gidney, M. Giustina, R. Graff, S. Habegger, A. Ho, S. Hong, T. Huang, L. B. Ioffe, S. V. Isakov, E. Jeffrey, Z. Jiang, C. Jones, D. Kafri, K. Kechedzhi, J. Kelly, S. Kim, P. V. Klimov, A. N. Korotkov, F. Kostritsa, D. Landhuis, P. Laptev, M. Lindmark, M. Leib, O. Martin, J. M. Martinis, J. R. McClean, M. McEwen, A. Megrant, X. Mi, M. Mohseni, W. Mruczkiewicz, J. Mutus, O. Naaman, C. Neill, F. Neukart, M. Y. Niu, T. E. O'Brien, B. O'Gorman, E. Ostby, A. Petukhov, H. Putterman, C. Quintana, P. Roushan, N. C. Rubin, D. Sank, A. Skolik, V. Smelyanskiy, D. Strain, M. Streif, M. Szalay, A. Vainsencher, T. White, Z. J. Yao, P. Yeh, A. Zalcman, L. Zhou, H. Neven, D. Bacon, E. Lucero, E. Farhi, and R. Babbush, Nature Physics **17**, 332 (2021).
- [23] D. Bertsimas and J. Tsitsiklis, Statistical Science **8**, 10 (1993).
- [24] D. Jungnickel, “The greedy algorithm,” in *Graphs, Networks and Algorithms* (Springer Berlin Heidelberg, Berlin, Heidelberg, 1999) pp. 129–153.
- [25] B. M. E. Moret, SIGACT News **19**, 51–54 (1988).
- [26] I. Dinur, O. Regev†, and C. Smyth‡, Combinatorica **25**, 519 (2005).
- [27] Michael Nielsen, *Neural Networks and Deep Learning* (Free Online Book, 2013).
- [28] N. Srivastava, G. Hinton, A. Krizhevsky, I. Sutskever, and R. Salakhutdinov, J. Mach. Learn. Res. **15**, 1929–1958 (2014).
- [29] T. Kadowaki and H. Nishimori, Phys. Rev. E **58**, 5355 (1998).
- [30] D. Aharonov, W. van Dam, J. Kempe, Z. Landau, S. Lloyd, and O. Regev, SIAM Journal on Computing **37**, 166 (2007).
- [31] A. Das and B. K. Chakrabarti, Rev. Mod. Phys. **80**, 1061 (2008).
- [32] A. Peruzzo, J. McClean, P. Shadbolt, M.-H. Yung, X.-Q. Zhou, P. J. Love, A. Aspuru-Guzik, and J. L. O'Brien, Nature Communications **5**, 4213 (2014).
- [33] A. Kandala, A. Mezzacapo, K. Temme, M. Takita, M. Brink, J. M. Chow, and J. M. Gambetta, Nature **549**, 242 (2017).
- [34] J. Tilly, H. Chen, S. Cao, D. Picozzi, K. Setia, Y. Li, E. Grant, L. Wossnig, I. Rungger, G. H. Booth, and J. Tennyson, arXiv e-prints , arXiv:2111.05176 (2021).
- [35] The scaling is partially due to the small Hamming distance of \hat{H}_B ; however, such locality is also the premise for arguments on quantum annealing, energy landscape, etc.
- [36] P. Jain and P. Kar, Foundations and Trends in Machine Learning **10**, 142 (2017).
- [37] J. R. McClean, S. Boixo, V. N. Smelyanskiy, R. Babbush, and H. Neven, Nature Communications **9**, 4812 (2018).
- [38] M. Cerezo, A. Sone, T. Volkoff, L. Cincio, and P. J. Coles, Nature Communications **12**, 1791 (2021).
- [39] S. Wang, E. Fontana, M. Cerezo, K. Sharma, A. Sone, L. Cincio, and P. J. Coles, Nature Communications **12**, 6961 (2021).
- [40] The saddle points and maximums are ruled out by the cost function.
- [41] M. Garey and D. Johnson, *Computers and Intractability: A Guide to the Theory of NP-completeness*, Mathematical Sciences Series (W. H. Freeman, 1979).
- [42] While most harder problems see a much lower R than the simpler ones, we cherry-pick those hardest ones with $R < 10\%$ for further analysis.